ATP-binding cassette member B5 (ABCB5) promotes tumor cell invasiveness in human colorectal cancer

Received for publication, April 4, 2018, and in revised form, April 23, 2018 Published, Papers in Press, May 22, 2018, DOI 10.1074/jbc.RA118.003187

Qin Guo,[a,b,c] Tanja Grimmig,[d] Gabriel Gonzalez,[a,b] Anita Giobbie-Hurder,[e] Gretchen Berg,[a,c] Nolan Carr,[a] Brian J. Wilson,[c,f,g] Pallavi Banerjee,[a,c] Jie Ma,[c] Jason S. Gold,[h,i] Bisweswar Nandi,[h,i] Qin Huang,[j] Ana Maria Waaga-Gasser,[d] Christine G. Lian,[k] George F. Murphy,[f,k] Markus H. Frank,[c,f,g] Martin Gasser,[d1] and Natasha Y. Frank[a,b,c,f1,2]

From the Departments of [a]Medicine, [i]Surgery, and [j]Pathology, Veterans Affairs Boston Healthcare System, Boston, Massachusetts 02132, the [b]Division of Genetics, [h]Department of Surgery, [k]Department of Pathology, and [g]Department of Dermatology, Brigham and Women's Hospital, Harvard Medical School, Boston, Massachusetts 02115, the [c]Transplant Research Program, Boston Children's Hospital, Harvard Medical School, Boston, Massachusetts 02115, the [d]Department of Surgery, University of Würzburg, 97070 Würzburg, Germany, the [e]Department of Biostatistics and Computational Biology, Dana-Farber Cancer Institute, Boston, Massachusetts 02115, and the [f]Harvard Stem Cell Institute, Harvard University, Cambridge, Massachusetts 02138

Edited by Xiao-Fan Wang

ABC member B5 (ABCB5) mediates multidrug resistance (MDR) in diverse malignancies and confers clinically relevant 5-fluorouracil resistance to CD133-expressing cancer stem cells in human colorectal cancer (CRC). Because of its recently identified roles in normal stem cell maintenance, we hypothesized that ABCB5 might also serve MDR-independent functions in CRC. Here, in a prospective clinical study of 142 CRC patients, we found that ABCB5 mRNA transcripts previously reported not to be significantly expressed in healthy peripheral blood mononuclear cells are significantly enriched in patient peripheral blood specimens compared with non-CRC controls and correlate with CRC disease progression. In human-to-mouse CRC tumor xenotransplantation models that exhibited circulating tumor mRNA, we observed that cancer-specific ABCB5 knockdown significantly reduced detection of these transcripts, suggesting that the knockdown inhibited tumor invasiveness. Mechanistically, this effect was associated with inhibition of expression and downstream signaling of AXL receptor tyrosine kinase (AXL), a proinvasive molecule herein shown to be produced by ABCB5-positive CRC cells. Importantly, rescue of AXL expression in ABCB5-knockdown CRC tumor cells restored tumor-specific transcript detection in the peripheral blood of xenograft recipients, indicating that ABCB5 regulates CRC invasiveness, at least in part, by enhancing AXL signaling. Our results implicate ABCB5 as a critical determinant of CRC invasiveness and suggest that ABCB5 blockade might represent a strategy in CRC therapy, even independently of ABCB5's function as an MDR mediator.

Tumor development and progression have been associated, at the DNA level, with cumulative alterations in oncogenes, tumor suppressor genes, and repair/stability genes (1, 2). At the cellular level, human cancers have been recognized to consist of phenotypically heterogeneous cell populations with variable ability for self-renewal and tumor propagation (3, 4). This observation led to the development of the cancer stem cell (CSC)[3] model of tumor initiation and growth (5), which has been broadly confirmed in multiple malignancies, including CRC (6–8). CSCs have been shown to contribute to the failure of existing therapies to consistently eradicate malignant tumors through diverse molecular mechanisms (9), including epithelial–mesenchymal transition (EMT) (10) associated with the ability of human cancers to invade the vasculature and disseminate to novel anatomic locations, leading to tumor progression and therapeutic resistance (11).

ABCB5 is a multidrug resistance (MDR) mediator expressed in diverse human malignancies (12), including CRC (13–15), where it is specifically overexpressed on therapy-resistant CD133(+) tumor subpopulations (16) previously found to represent CSC (6–8). ABCB5 confers CRC drug resistance to 5-fluorouracil (14, 16). Whether ABCB5 might also serve a drug resistance–independent function in CRC, a possibility raised by recent studies in Abcb5-knockout (KO) mice that revealed key functions of this molecule in stem cell maintenance in nonmalignant tissues (17), is currently unknown.

This work was supported by Veterans Affairs Grants BLR&D 1I01BX000516 and RR&D 1I01RX000989 Merit Review Awards and a Department of Defense translational team science award (to N. Y. F.) and NCI, National Institutes of Health, Grants R01CA113796, R01CA158467, and R01CA138231 (to M. H. F.). N. Y. F. and M. H. F. are co-inventors of the ABCB5-related United States patent 7,928,202 (Targeting ABCB5 for cancer therapy) assigned to Brigham and Women's Hospital (Boston, Massachusetts) and licensed to Ticeba GmbH (Heidelberg, Germany) and Rheacell GmbH & Co. KG (Heidelberg, Germany). M. H. F. serves as a scientific advisor to Ticeba GmbH and Rheacell GmbH & Co. KG. The content is solely the responsibility of the authors and does not necessarily represent the official views of the National Institutes of Health.
This article contains Tables S1 and S2.
[1] Co-senior investigators.
[2] To whom correspondence should be addressed: Veterans Affairs Boston Healthcare System, 1400 VFW Pkwy., Boston, MA 02132. Tel.: 617-525-4451; Fax: 617-525-5333; E-mail: nyfrank@bwh.harvard.edu.

[3] The abbreviations used are: CSC, cancer stem cell; UICC, Union for International Cancer Control; EMT, epithelial–mesenchymal transition; MDR, multidrug resistance; KO, knockout; OS, overall survival; CI, confidence interval; HR, hazard ratio; shRNA, short hairpin RNA; KD, knockdown; GAPDH, glyceraldehyde-3-phosphate dehydrogenase; IL, interleukin; FBS, fetal bovine serum.

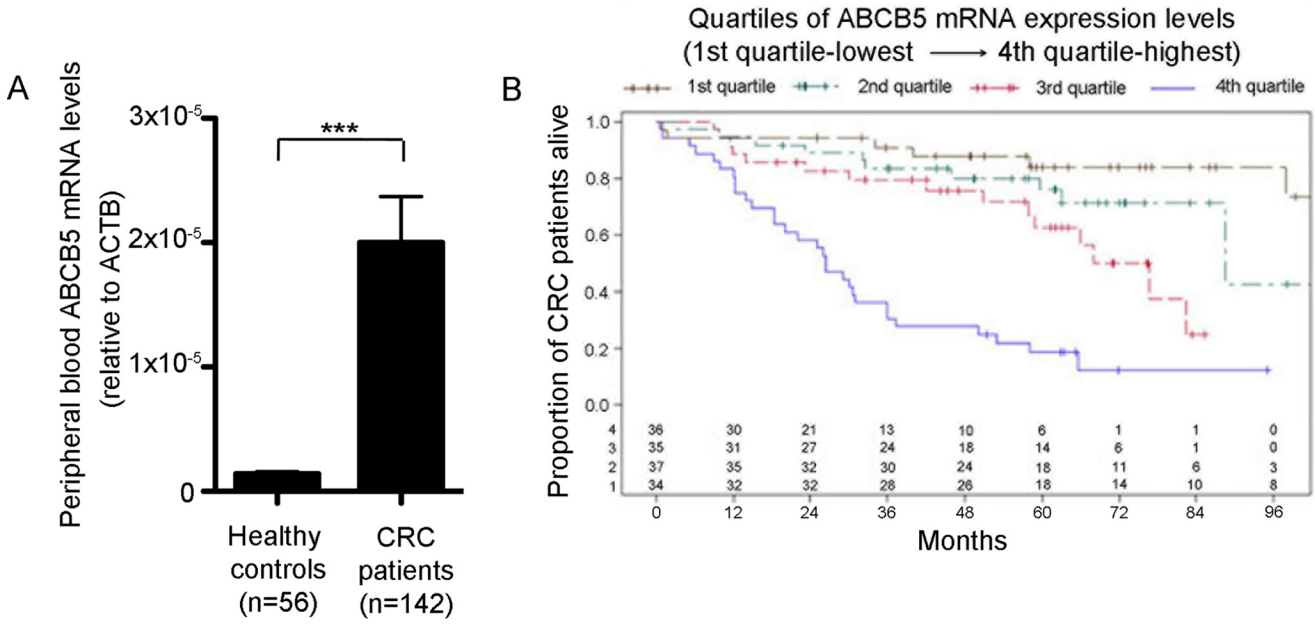

Figure 1. ABCB5 as a prognostic marker in CRC. *A*, comparison of ABCB5 mRNA expression in PBMCs of CRC patients and healthy controls. Data were analyzed using the unpaired *t* test. *Error bars*, S.E. ***, $p < 0.001$. *B*, evaluation of OS according to quartiles of ABCB5 mRNA expression in PBMCs of CRC patients. The distributions of OS were summarized using the Kaplan–Meier method with 95% CIs estimated using log (−log(end point)) methodology.

Colorectal cancer CSC can be identified by a number of molecular markers, including CD133 (6–8), ALDH1 (18), LGR5 (19), and LRIG1 (20). Several studies have shown that high expression of CSC markers in primary tumors could serve as a predictor of poor prognosis (reviewed in Refs. 21–23) in CRC. In the current study, we hypothesized that drug transport–independent functions of ABCB5, first discovered in nonmalignant tissue-specific stem cells (17), might also be relevant to malignant disease, in particular human CRC, where a requirement of ABCB5 for more efficient tumorigenic growth had previously been identified (16). Here, we first identified a potential role of ABCB5 in CRC invasiveness in human CRC patients, where ABCB5 mRNA levels detected in the peripheral blood markedly exceeded baseline threshold levels in healthy controls and served as an independent predictor of poor overall survival (OS).

In human-to-mouse CRC tumor xenotransplantation models that exhibited circulating tumor mRNA, we found that cancer-specific ABCB5 knockdown significantly reduced detectability of these transcripts, suggesting inhibition of tumor invasiveness through cancer-specific ABCB5 knockdown. Mechanistically, this effect was associated with inhibition of expression and downstream signaling of the receptor tyrosine kinase AXL, a pro-invasive molecule herein shown to be produced by ABCB5-positive CRC cells. Importantly, rescue of AXL expression in ABCB5-knockdown CRC tumor cells restored tumor-specific transcript detection in the peripheral blood of xenograft recipients, indicating that ABCB5 regulates CRC invasiveness, at least in part, through enhancement of AXL signaling. Our results implicate ABCB5 as a novel determinant of CRC invasiveness and suggest that ABCB5 blockade might represent a novel strategy for CRC therapy, even in settings independent of its function as an MDR mediator.

Results

Peripheral blood circulating ABCB5 mRNA levels are associated with poor OS in CRC

CSCs have been associated with increased cancer virulence and deemed responsible for cancer metastatic progression and reduced patient survival (12, 24). Based on our prior studies, which indicated that ABCB5 marks aggressive CSC in human CRC (16), we evaluated whether ABCB5 mRNA expression in peripheral blood specimens of patients with CRC correlates with poor prognosis. This study was conducted in a prospective cohort of 142 CRC patients undergoing treatment at the University of Würzburg Hospital (Table S1). Peripheral blood specimens obtained from enrolled CRC patients before treatment initiation and from age-matched healthy controls were evaluated for ABCB5 mRNA expression. The analyses were performed using RNA isolated from all circulating cells collected by centrifugation. Because ABCB5 is expressed only at extremely low or undetectable levels in normal mononuclear blood cells (25, 26), we posited that ABCB5 mRNA detectability in the peripheral blood of CTC patients might serve as an initial measure for assessment of tumor invasiveness in a clinical setting, as has been shown in other ABCB5-expressing cancers (26). In this study, we found significant enrichment of ABCB5 mRNA transcripts in CRC patients compared with healthy controls ($p < 0.0001$; Fig. 1*A*). Moreover, peripheral blood ABCB5 mRNA levels were significantly associated with tumor location, UICC stage, N stage, and M stage (Table S2). Additionally, using the Kaplan–Meier method and the Cox model, we determined that peripheral blood ABCB5 mRNA levels served as an independent predictor of OS in CRC patients. ABCB5 expression values were hereby divided into four classes according to the quartiles of the distribution: from the first quartile (lowest expression levels) to the fourth quartile (highest expression

Table 1
Median OS times according to quartiles of ABCB5 expression

ΔCt values	Median	Lower 95% CI	Upper 95% CI
4th quartile: $\Delta Ct < 15.808$	26.4	18.3	36.0
3rd quartile: $15.808 < \Delta Ct < 16.92725$	76.7	57.9	∞
2nd quartile: $16.92725 < \Delta Ct < 18.2935$	88.5	88.4	∞
1st quartile: $\Delta Ct > 18.2935$	Not reached		

Table 2
OS Cox model results according to the quartiles of ABCB5 expression

Predictor	Hazard ratio	Lower 95% CI	Upper 95% CI	*p* value
ABCB5				0.0003
ABCB5 quartile 3 *versus* 4	0.50	0.23	1.06	
ABCB5 quartile 2 *versus* 4	0.25	0.11	0.58	
ABCB5 quartile 1 *versus* 4	0.13	0.05	0.35	
UICC				0.02
UICC stage 2 *versus* 1	1.02	0.49	2.15	
UICC stage 3 *versus* 1	0.72	0.33	1.60	
UICC stage 4 *versus* 1	2.60	1.02	6.61	

levels). The distributions of OS were summarized using the Kaplan–Meier method with 95% confidence intervals (CIs) estimated using the log (−log(end point)) methodology. The Kaplan–Meier curves and Cox model results revealed significant differences in OS for the different levels of ABCB5 expression, with the highest quartile of expression having the poorest OS. Median OS in the group with the highest ABCB5 expression was 26 months, compared with at least 76 months in the lower quartiles (Fig. 1*B* and Table 1). The Cox model suggested two important predictors of OS in this cohort of patients: ABCB5 and UICC stage (Table 2). Compared with patients with the highest ABCB5 expression levels (fourth quartile), patients in quartiles 1 and 2 with lower ABCB5 expression showed significant reductions of 87 and 75%, respectively, in the hazards of death (HR 0.13 and 95% CI 0.05–0.35; HR 0.25 and 95% CI 0.11–0.58). Additionally, patients with UICC stage 4 had significant increases in the hazard of death compared with UICC stage 1 (HR 2.6 and 95% CI 1.02–6.6). These results suggested that ABCB5 might represent a novel predictor of poor OS in CRC patients and pointed to a potential functional role of ABCB5 in CRC invasiveness, providing a rationale for further dissection of ABCB5-dependent invasiveness in experimental model systems.

ABCB5 expression is enhanced in metastatic CRC cells

Based on our finding of enhanced ABCB5 mRNA expression in the peripheral blood of CRC patients as opposed to controls and the correlation of CRC ABCB5 expression with patient outcome, we hypothesized that human CRC cells with enhanced metastatic potential overexpressed ABCB5. We found that a cell line (SW620) derived from a metastatic lesion of a CRC patient expressed significantly higher levels of ABCB5 than one (SW480) derived from the primary tumor of the same patient (Fig. 2*A*, SW620 *versus* SW480: 15.2 ± 2.3% *versus* 10.6 ± 1.9% cell positivity, $p < 0.05$, mean ± S.E.). This finding was experimentally recapitulated when examining in a CRC xenotransplantation model ABCB5 expression in COLO741 cells (a CRC cell line selected for its known metastatic potential) that had metastasized to the lung (COLO741MET) as opposed to COLO741 cells re-isolated from the primary tumor lesion (Fig. 2*B*, COLO741MET *versus* COLO741: 27.0 ± 3.4% *versus* 16.5 ± 3.3% cell positivity, $p < 0.01$, mean ± S.E.).

ABCB5 is required for tumor vascular invasion

Next, we utilized an established human-to-NSG mouse subcutaneous CRC tumor xenotransplantation model (6, 7) to compare *in vivo* the vascular invasion potential of the COLO741MET *versus* the COLO741 cell line (Fig. 3*A*). This was accomplished by measuring tumor-derived, human-specific mRNA transcripts (*i.e.* glyceraldehyde-3-phosphate dehydrogenase (GAPDH), B2M, PPIA, and MRPL19) (27) in murine peripheral blood samples harvested 8 weeks after primary tumor inoculation. We found that all four human CRC-derived mRNA transcripts were significantly enriched in the peripheral blood of mice injected with COLO741MET cells compared with mice injected with COLO741 cells (Fig. 3*B*). At this time point, primary tumors in COLO741MET-injected mice had reached a mean volume of 605.4 ± 40.7 mm^3, and tumors in COLO741-injected mice had reached a mean volume of 250.2 ± 28.1 mm^3 ($n = 8$ mice/group, $p < 0.001$, mean ± S.E.). To test whether this enhanced vascular invasion was driven by ABCB5 overexpression, we performed shRNA-mediated ABCB5 knockdown (ABCB5 KD) in COLO741MET cells, which resulted in a >90% inhibition of ABCB5 mRNA expression and an ~50% reduction of ABCB5 protein expression due to relatively high ABCB5 protein stability in line with previous findings (28) (Fig. 3*C*, *top panels*). Whereas ABCB5 KD in human malignancies, including CRC, is known to inhibit primary tumor growth (16), and whereas in the current study primary tumors in COLO741MET ABCB5 KD–injected mice were accordingly smaller than tumors injected with COLO741MET CONTROL cells (263.4 ± 47.5 *versus* 662.8 ± 66.1 mm^3, $n = 7$ mice/group, $p < 0.001$, mean ± S.E.), there exists no known correlation between primary tumor size and the development of metastasis in experimental cancer xenotransplantation models or even in clinical findings in CRC patients (29, 30). Thus, examination of tumor invasiveness at a specific time point was warranted. Compared with COLO741MET cells transfected with a control plasmid (COLO741MET CONTROL), mice xenografted with COLO741MET ABCB5-KD cells exhibited significantly reduced levels of human mRNA transcripts in their peripheral blood at 8 weeks after tumor inoculation (Fig. 3*C*, *bottom panels*), indicating that the enhanced invasion potential of COLO741MET tumor cells depends on functional ABCB5.

To further investigate whether ABCB5-dependent metastatic propensity *in vivo* resulted from a role of the molecule in CRC invasiveness, we utilized an established *in vitro* trans-well assay to study the invasive capacity of WT *versus* ABCB5-KD cell subsets and to examine the effect of monoclonal antibody (mAb)-mediated ABCB5 blockade on the invasiveness of CRC cells. First, consistent with our *in vivo* results, we found a significantly higher invasiveness of COLO741MET cells compared with COLO741 cells (invading cell numbers of COLO741MET *versus* COLO741 cells: 139.3 ± 15.1 *versus* 85.3 ± 11.1 cells, $p < 0.05$, mean ± S.E.) (Fig. 3*D*). This higher invasive capacity of COLO741MET cells was inhibited by shRNA-mediated ABCB5 knockdown, with a significant reduction of invading cell numbers in COLO741MET ABCB5-KD

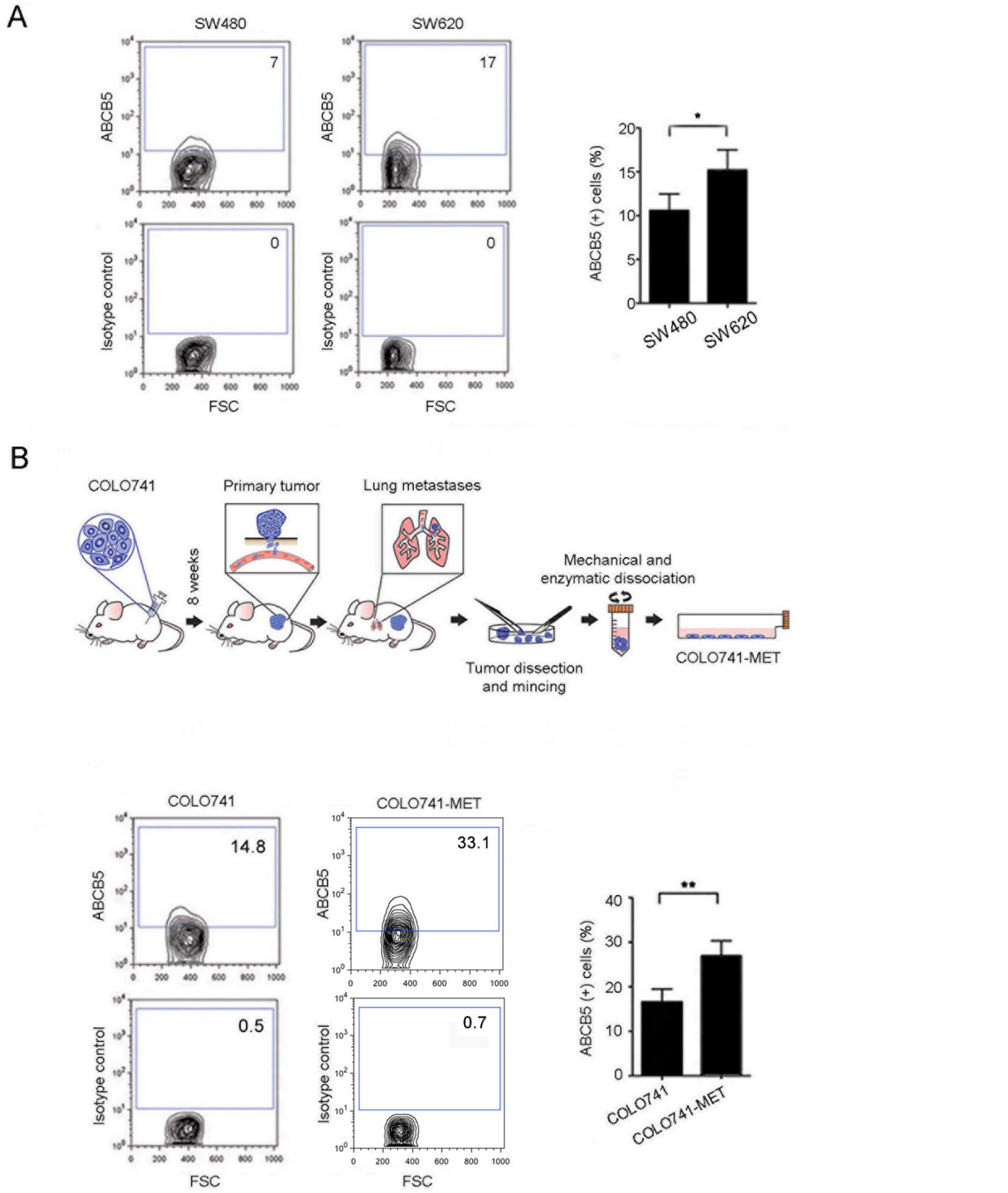

Figure 2. Comparative analyses of ABCB5 expression in primary and metastatic CRC cell lines. Representative ABCB5 flow cytometry analyses of the primary tumor-derived SW480 and metastasis-derived SW620 cell lines (*A*) and the parental COLO741 and metastatic COLO741MET cell lines (*B*, *bottom*) are shown. *B*, *top*, *schematic illustration* of the generation of the metastatic COLO741MET cell line. *Bar graphs* in *A* and *B* depict the comparative quantitative analyses of ABCB5 positivity. Each experiment was performed three times. Data were analyzed using the unpaired *t* test. *Error bars*, S.E. *, $p < 0.05$; **, $p < 0.01$.

cultures compared with COLO741MET CONTROL cultures (COLO741MET ABCB5 KD *versus* COLO741MET CONTROL: 59.3 ± 14.2 *versus* 170.0 ± 36.6 cells, $p < 0.05$, mean ± S.E.) (Fig. 3*D*). A similar effect was observed in the setting of mAb-mediated ABCB5 blockade (17, 25, 31), which resulted in >90% inhibition of the invasiveness of COLO741MET cells and, similarly, in >90% inhibition of the invasiveness of additionally examined human SW620 cells derived from a metastatic lymph node of a CRC patient (ABCB5 mAb *versus* isotype control treatment: 2.3 ± 0.6 *versus* 160.7 ± 1.2 cells, $p < 0.001$, mean ± S.E., COLO741MET; 7.3 ± 1.3 *versus* 102.3 ± 27.2 cells, $p < 0.05$, mean ± S.E., SW620) (Fig. 3*D*). Taken together, those findings revealed a novel role of ABCB5 in regulating CRC cell invasiveness in the specimens under study.

ABCB5 promotes epithelial mesenchymal transition in CRC

EMT has been shown to play a critical role in enabling cancer tissue invasion through transitioning from a less aggressive, epithelial, to a more aggressive, mesenchymal, phenotype (10). Based on our findings that ABCB5 is required for CRC cell

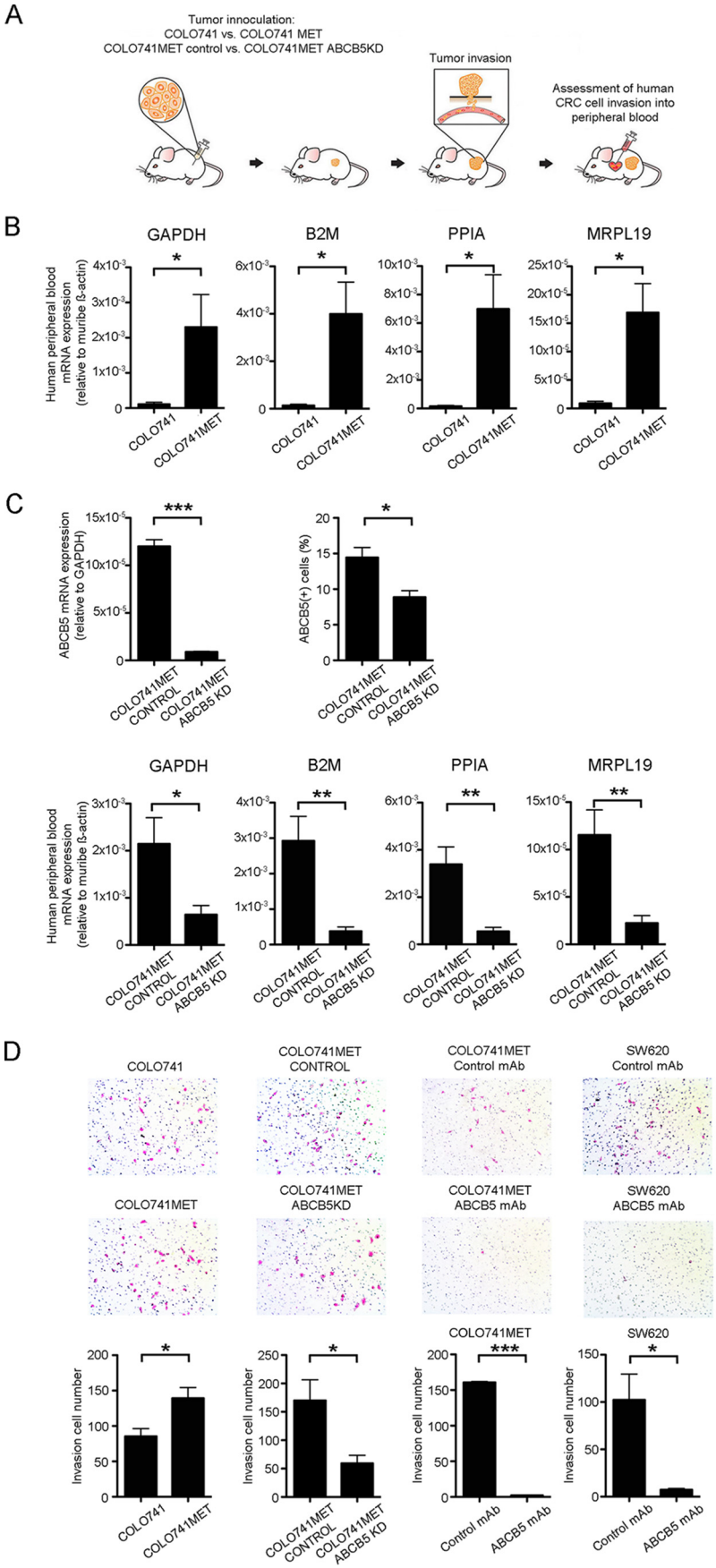
A
Tumor innoculation:
COLO741 vs. COLO741 MET
COLO741MET control vs. COLO741MET ABCB5KD
Tumor invasion
Assessment of human CRC cell invasion into peripheral blood
B
GAPDH
B2M
PPIA
MRPL19
Human peripheral blood mRNA expression (relative to muribe ß-actin)
COLO741
COLO741MET
C
ABCB5 mRNA expression (relative to GAPDH)
ABCB5(+) cells (%)
COLO741MET CONTROL
COLO741MET ABCB5 KD
D
COLO741
COLO741MET CONTROL
COLO741MET Control mAb
SW620 Control mAb
COLO741MET
COLO741MET ABCB5KD
COLO741MET ABCB5 mAb
SW620 ABCB5 mAb
Invasion cell number
Control mAb
ABCB5 mAb

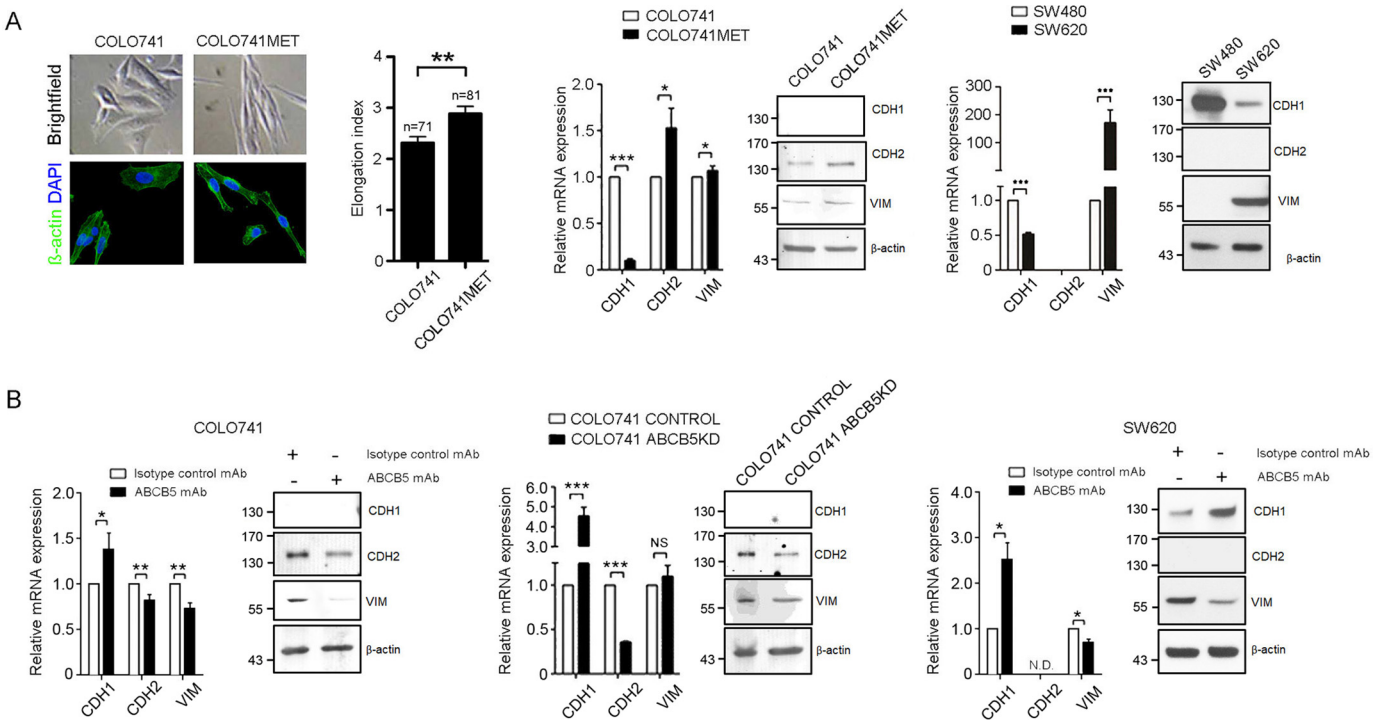

Figure 4. Role of ABCB5 in mesenchymal phenotype maintenance. *A*, representative images of cultured COLO741 and COLO741MET cells. Bright field microscopy images are shown in the *top panels*, and immunofluorescent β-actin–stained images (*green*) are shown in the *bottom panels*. Nuclei were stained with 4′,6-diamidino-2-phenylindole (DAPI) (*blue*). The *bar graph* depicts the quantitative morphometric analysis of cellular elongation, which was computed as Max Feret per Min Feret (the maximum and minimum length, respectively, for all orientations) on the single cell using NIS-Elements Viewer software. Comparative analyses of epithelial (CDH1) and mesenchymal (CDH2 and VIM) marker expression in COLO741 *versus* COLO741MET and in SW480 *versus* SW620 are shown on the *right*. *B*, effect of mAb- or shRNA-mediated ABCB5 blockade on CDH1, CDH2, and VIM expression in COLO741 and SW620 cells as determined by real-time RT-PCR and Western blotting. Data were analyzed using the unpaired *t* test. *Error bars*, S.E. *, $p < 0.05$; **, $p < 0.01$; ***, $p < 0.001$.

invasion and hematological spread, we hypothesized that ABCB5 expression is associated with EMT and might regulate the mesenchymal cellular phenotype in CRC. First, we found that morphologically, in contrast to *in vivo*-unpassaged, parental COLO741 cells that exhibited flattened and polygonal shapes consistent with epithelial cell characteristics (Fig. 4*A*), COLO741MET cells with higher ABCB5 expression (as shown in Fig. 2*B*) appeared smaller, spindle-shaped, and significantly more elongated ($p < 0.01$) with tapering cytoplasmic poles consistent with a mesenchymal phenotype (Fig. 4*A*). In line with an EMT phenotype, COLO741MET cells expressed lower mRNA levels of the epithelial marker E-cadherin (CDH1) and higher mRNA levels of the mesenchymal markers N-cadherin (CDH2) and vimentin (VIM) compared with parental COLO741 cells (Fig. 4*A*). Western blot analyses also revealed high protein levels for CDH2 and VIM in COLO741MET *versus* COLO741 cells (Fig. 4*A*), whereas CDH1 protein was undetectable by Western blotting in either cell line. Similarly, patient metastatic lymph node–derived SW620 cells also expressed higher levels of VIM and lower levels of CDH1 compared with their SW480 counterparts derived from the primary colonic adenocarcinoma of the same patient at both mRNA and protein levels (Fig. 4*A*). In both SW480 and SW620 cell lines, CDH2 was not detectable at the mRNA or the protein levels (Fig. 4*A*).

Next, we examined whether ABCB5 is required for the maintenance of the mesenchymal phenotype in CRC cells using either mAb- or shRNA-mediated ABCB5 blockade. ABCB5 inhibition in COLO741 cells through either mAb treatment or ABCB5 KD resulted in attenuated expression of CDH2 and VIM and enhanced expression of CDH1 at the mRNA level and in attenuated CDH2 and VIM expression at the protein level, whereas CDH1 was not detectable at the protein level in either ABCB5 blockade or control cultures (Fig. 4*B*). Similar reciprocal changes in epithelial and mesenchymal marker expression were observed as a result of mAb-based ABCB5 blockade in the metastatic cell line SW620, which also exhibited enhanced

Figure 3. ABCB5 maintains an invasive cell phenotype in human CRC cells. *A*, *schematic illustration* of the *in vivo* tumor invasion assay. *Bar graphs*, comparison of relative human GAPDH, B2M, PPIA, and MRPL19 mRNA levels in PBMCs of mice injected subcutaneously with either COLO741 or COLO741MET cells ($n = 7$ mice/group) (*B*) or with COLO741MET CONTROL or COLO741MET ABCB5-KD cells ($n = 6$ mice/group) (*C*, *bottom*). *C*, *top*, generation of the COLO741MET ABCB5-KD cell line. The *bar graph* on the *right* depicts ABCB5 mRNA expression relative to human GAPDH mRNA levels in COLO741MET CONTROL *versus* COLO741MET ABCB5-KD cells; the overall quantitative analyses of ABCB5 positivity by flow cytometry are shown on the *right*. Data were analyzed using the unpaired *t* test. *Error bars*, S.E. *D*, *in vitro* cell invasion assays for COLO741 *versus* COLO741MET and COLO741MET CONTROL *versus* COLO741MET ABCB5-KD cell lines and *in vitro* cell invasion assays for COLO741MET and SW620 cells treated with either isotype control mAb or ABCB5 mAb. All studies were conducted in triplicates. Representative images of invading Diff-Quik–stained cells (*pink*) are shown in the respective *top panels*. *Bar graphs* in the *bottom panels* illustrate mean numbers of invading cells per well ($n = 3$ independent experiments, each replicate representing sums of invading cells detected in 4 randomly chosen microscopic fields/well). Data were analyzed using the unpaired *t* test. *Error bars*, S.E. *, $p < 0.05$; **, $p < 0.01$; ***, $p < 0.001$.

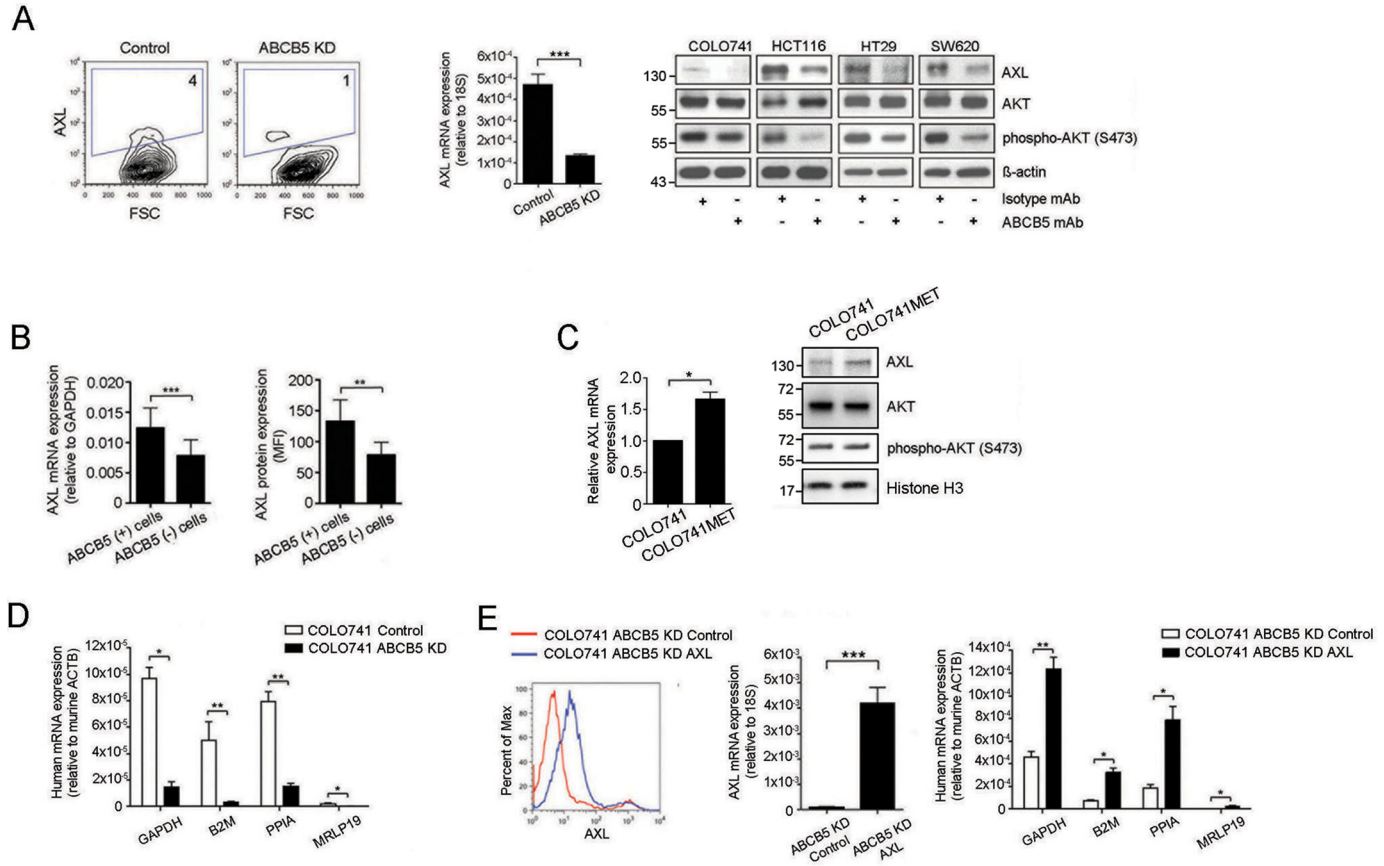

Figure 5. ABCB5(+) CRC cells express the EMT-sustaining receptor tyrosine kinase AXL, which serves as a mediator of ABCB5-dependent cancer invasion. *A* (*left*), a representative flow cytometric analysis of AXL protein expression in an ABCB5-KD *versus* a control-transfected cell line. The *bar graph* illustrates AXL mRNA expression in ABCB5-KD *versus* control-transfected human CRC cells. *A* (*right*), Western blot analyses of AXL, AKT, and phospho-AKT protein expression in either anti-ABCB5 mAb-treated or isotype control-treated CRC cells. *B*, *bar graphs* depict comparative AXL mRNA and protein expression of sorted ABCB5(+) *versus* ABCB5(−) cells isolated from COLO741, SW620, HT29, or HCT116 CRC cells, as determined by quantitative RT-PCR analyses (*left*) and flow cytometry (*right*). For each cell line, triplicate samples were tested. Data analysis was performed using the paired *t* test. *C*, the *bar graph* illustrates AXL mRNA expression in COLO741 *versus* COLO741MET cells. Western blot analyses of AXL, AKT, and phospho-AKT protein expression are shown on the *right*. *D*, shRNA-mediated ABCB5 KD results in reduced tumor invasion *in vivo*. The *bar graph* depicts the comparison of relative human GAPDH, B2M, PPIA, and MRPL19 mRNA levels in PBMCs of mice injected subcutaneously with either ABCB5-KD or control-transfected COLO741 cells (n = 9 mice/group). *E* (*left*), exogenous overexpression of AXL in ABCB5-KD cells. Representative flow cytometry analysis of AXL protein expression in ABCB5-KD control–transfected (*red*) *versus* ABCB5-KD AXL–transfected (*blue*) cells. The *bar graph* depicts AXL mRNA expression in ABCB5-KD control–transfected *versus* ABCB5-KD AXL–transfected CRC cells. *E* (*right*), AXL restores tumor cell invasion in the setting of ABCB5 blockade. The *bar graph* depicts the comparison of relative human GAPDH, B2M, PPIA, and MRPL19 mRNA levels in PBMCs of mice injected subcutaneously with either AXL-overexpressing ABCB5-KD (n = 4 mice per group) or control-transfected ABCB5-KD COLO741 cells (n = 6 mice/group). Data were analyzed using unpaired *t*-tests. *Error bars*, S.E. *, $p < 0.05$; **, $p < 0.01$; ***, $p < 0.001$.

CDH1 and reduced VIM mRNA and protein expression in ABCB5 mAb–treated compared with isotype control–treated cultures (Fig. 4*B*). These results revealed a novel functional role of ABCB5 in the maintenance of a mesenchymal phenotype in human CRC cells and provided proof of principle that this phenotype can be targeted through ABCB5 mAb blockade in a translationally relevant manner.

ABCB5 promotes tumor invasion through regulation of AXL

Recent studies have shown that the receptor tyrosine kinase AXL, which correlates with adverse CRC prognosis (32), is responsible for EMT induction in other malignancies (33, 34). We found that AXL mRNA expression was diminished in COLO741 ABCB5-KD CRC cell cultures by >90% and that AXL protein expression was reduced in these cells by >50% compared with control-transfected cells (Fig. 5*A*). Furthermore, mAb-mediated ABCB5 blockade consistently inhibited expression of AXL in all of four CRC cell lines examined (COLO741, SW620, HT29, and HCT116, with ABCB5(+) tumor cell frequencies ranging from 9 to 27%), as determined by Western blot analysis (Fig. 5*A*), and also inhibited, to a lesser degree, its downstream target phospho-AKT. The functional relationship between ABCB5 and AXL was supported by significantly up-regulated AXL expression at both mRNA and protein levels in untreated ABCB5(+) cells sorted from all four cell lines by flow cytometry (Fig. 5*B*). Moreover, AXL expression (as determined at both mRNA and protein levels) and downstream signaling (phospho-AKT/AKT ratios) were enhanced in metastasis-derived COLO741MET *versus* parental COLO741 cells (Fig. 5*C*). To investigate whether ABCB5-driven CRC invasiveness is mediated by AXL *in vivo*, we examined whether AXL overexpression in COLO741 ABCB5-KD cells could restore hematological cancer dissemination in an established human-to-NSG mouse subcutaneous tumor xenotransplantation model (6, 7), in which mice were grafted with either COLO741 ABCB5-KD cells or their respective controls or COLO741 ABCB5-KD cells trans-

fected with AXL or their respective controls. Murine recipient peripheral blood samples were collected 16 weeks after tumor inoculation and examined for expression of human-specific GAPDH, B2M, PPIA, and MRPL19 mRNA transcripts (27). We found that human cancer-derived mRNA transcript levels were significantly reduced in peripheral blood samples of NSG mice transplanted with COLO741 ABCB5-KD cells compared with controls (Fig. 5*D*). Moreover, exogenous restoration of AXL expression in ABCB5-KD cells (Fig. 5*E*, *left* and *center*) significantly reversed this effect (Fig. 5*E*, *right*). Taken together, these results indicated that ABCB5-driven hematological CRC dissemination is mediated, at least in part, through regulation of AXL.

ABCB5-mediated EMT induction depends on an IL-8/AXL signaling cascade

Previous studies revealed a critical role of IL-8 in the induction of CRC EMT (35, 36). Based on our discovery of a novel functional relationship between ABCB5 and AXL and on the established molecular role of ABCB5 in IL-8 production (13), we hypothesized that ABCB5 might also employ the IL-8 pathway to sustain AXL-mediated EMT in CRC. To test this hypothesis, we first examined the effect of ABCB5 blockade on IL-8 production by CRC cells. We found that ABCB5 mAb treatment resulted in a significant reduction of IL-8 production in all four CRC cell lines examined (Fig. 6*A*, *left*). A similar effect was observed in the setting of shRNA-mediated ABCB5 KD, tested in an exemplary manner in COLO741 cells (Fig. 6*A*, *right*). Additionally, exogenous administration of recombinant IL-8 reversed ABCB5 mAb-induced inhibition of AXL expression in HCT116, HT29, SW620, and COLO741 CRC cell cultures (Fig. 6*B*), as evidenced by quantitative ImageJ-based densitometry analyses of the Western blotting data, which revealed significant IL-8–induced augmentation of AXL levels compared with the impaired levels (63 ± 6% inhibited, $p < 0.01$, mean ± S.E.) observed in ABCB5-blocked cultures, by 40% ± 18%, $p < 0.05$, mean ± S.E., at 1 ng/ml IL-8 concentrations, indicating that ABCB5 control of AXL expression is mediated, at least in part, via IL-8. Moreover, exogenous administration of recombinant IL-8 was also associated with restoration of mesenchymal marker expression (CDH2 and VIM in COLO741 cells and VIM in SW620 cells; Fig. 6*C*) and inhibition of epithelial marker expression (CDH1) in SW620 cells (Fig. 6*C*). Specifically, quantitative ImageJ-based densitometry analyses of the Western blotting data showed a significant IL-8–induced dose-dependent increase in CDH2 and VIM (up to 68 and 90%, respectively, at 1 ng/ml IL-8 concentration, $p < 0.05$), compared with the impaired levels of CDH2 (77% inhibited) and VIM (85% inhibited) observed in ABCB5-blocked COLO741 cultures (Fig. 6*C*, *left*). Similar results were observed in SW620 cultures, where quantitative Western blot analyses showed a significant IL-8–induced dose-dependent increase in VIM (up to 30% at 1 ng/ml IL-8 concentration, $p < 0.05$) compared with the impaired levels of VIM (62% inhibited) observed in ABCB5-blocked cultures (Fig. 6*C*, *right*). In addition, SW620 cultures exhibited IL-8–induced dose-dependent attenuation of epithelial marker CDH1 expression (75% inhibited) at 1 ng/ml IL-8 concentration ($p < 0.05$), compared with the 35% augmentation of CDH1 observed in the setting of ABCB5 blockade (Fig. 6*C*, *right*). These results indicate that ABCB5 control of EMT marker expression is also mediated, at least in part, via IL-8.

Discussion

Previously, ABCB5 has been shown to represent a clinically relevant MDR mechanism, based on drug efflux function, in diverse human malignancies (13, 16, 37–39), which can be therapeutically targeted in CSC subpopulations through mAb-mediated functional blockade that inhibits ABCB5-mediated drug efflux or through therapeutic ablation of ABCB5-expressing, drug-effluxing CSCs via antibody-dependent cell-mediated cytotoxicity (31, 37). In contrast, drug efflux-independent functions of ABCB5 in CSC and normal tissue-specific stem cells are only beginning to be elucidated. For example, ABCB5 has been shown to control a pro-inflammatory cytokine signaling axis involving IL-8 production and IL-8–dependent CSC maintenance in human melanoma (13) and to exert anti-apoptotic functions in normal tissue-specific stem cells through p53 stabilization and regulation of BCL-2/BCL-X expression (17).

In CRC, ABCB5 has been shown to confer therapeutic resistance to 5-fluorouracil (14, 16), and ABCB5-mediated chemoresistance has been found to be positively regulated by c-MYC (14), whereas microRNA-522 could reverse ABCB5-mediated drug resistance as a negative regulator of ABCB5 expression (15). However, drug resistance–independent functions of ABCB5 in CRC have not been reported before our current study.

Here, using gene knockdown– and mAb–based ABCB5 inhibition strategies *in vitro* or ABCB5 blockade in tumor xenotransplantation models *in vivo*, we demonstrate for the first time that ABCB5 controls CRC cell invasiveness, unrelated to its previously established function as a drug resistance mechanism.

Mechanistically, we show that this novel function involves, at least in part, ABCB5-mediated control of IL-8 production paralleling findings previously established in melanoma (13) and, additionally, a downstream pathway of IL-8–dependent induction of AXL, a receptor tyrosine kinase with known roles in CRC invasiveness (32). Consistent with these results, we provide initial evidence for a role of ABCB5 in the EMT phenotype of colorectal cancer cells, which has also been previously linked to tumor invasiveness, including in CRC (40). Thus, our study implicates ABCB5 as a novel link between drug resistance, EMT, and tumor invasiveness in CRC, with potentially important implications for CRC therapy and prognosis. For example, the ABCB5-regulated downstream molecules IL-8 and AXL confer tumor resistance to EGFR-targeted therapies (41–43), which are widely used for the treatment of advanced CRC (44–46). Further exploration of ABCB5 as a potential novel target to sensitize EGFR-resistant CRC tumors to therapy might therefore be warranted. With regard to the potential relevance of our findings to clinical CRC progression and prognosis, we found in an initial clinical study a specific association between increased circulating ABCB5 mRNA levels and poor OS in CRC patients. This result parallels previous findings in clinical melanoma, where circulating ABCB5 mRNA levels had significant prognostic value in inferring disease recurrence (26). Importantly,

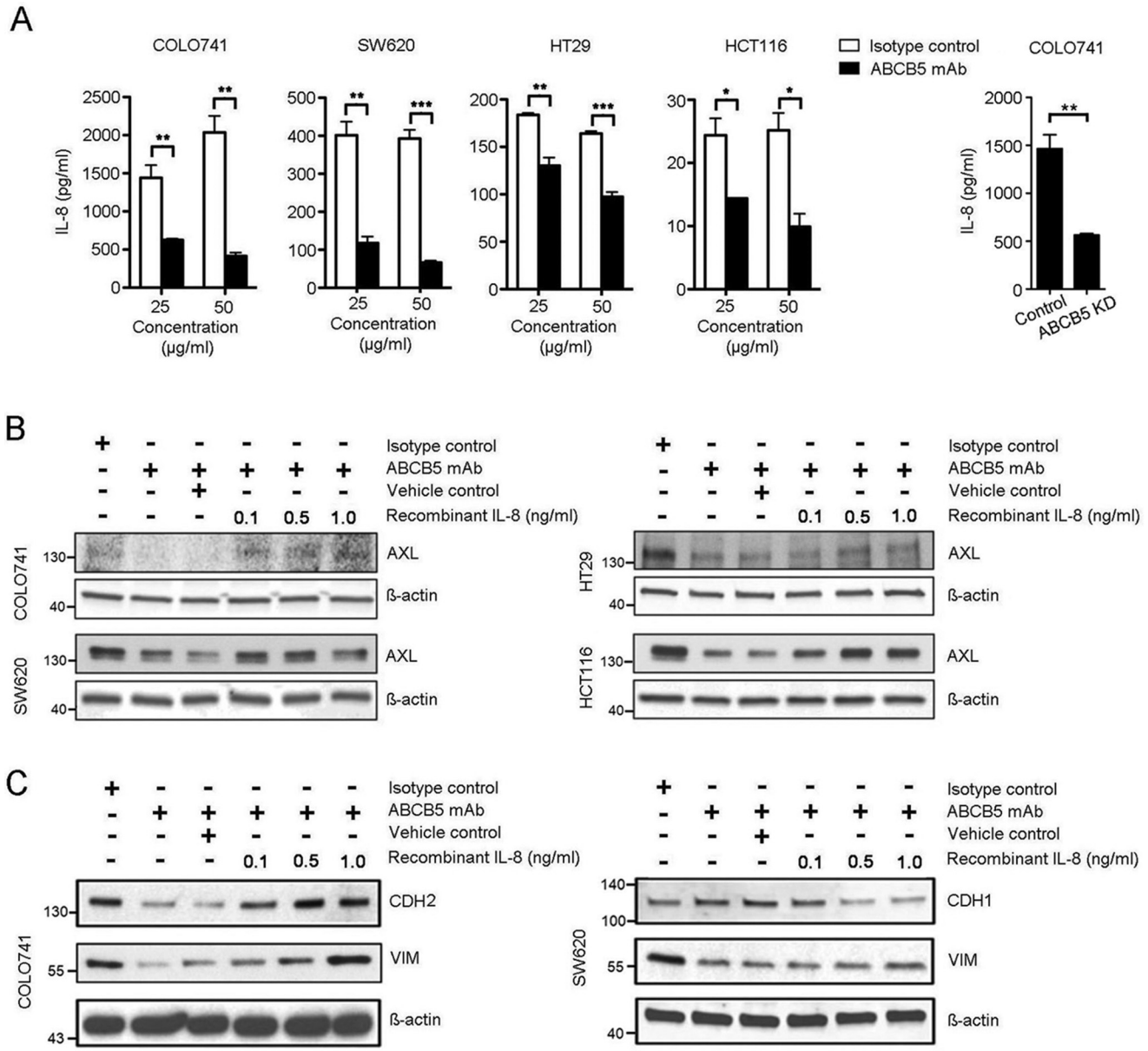

Figure 6. ABCB5-mediated EMT induction depends on IL-8/AXL signaling cascade. *A* (*left*), effect of mAb-mediated ABCB5 blockade on IL-8 secretion by CRC cells. *Bar graphs* represent comparative quantitative analyses of IL-8 concentrations in culture supernatants obtained from CRC cells treated with either ABCB5 mAb or isotype control mAb (25 or 50 μg/ml) as determined by ELISAs. All studies were conducted in triplicates. The data were analyzed using two-way analysis of variance. *Error bars*, S.E. *, $p < 0.05$; **, $p < 0.01$; ***, $p < 0.001$. *A* (*right*), effect of ABCB5 KD on IL-8 secretion by COLO741 cells. The *bar graph* depicts comparative quantitative analyses of IL-8 in culture supernatants obtained from COLO741 or COLO741 ABCB5-KD cells as determined by ELISAs. The data were analyzed using unpaired *t* test. *Error bars*, S.E. **, $p < 0.01$. *B*, Western blot analyses of AXL expression in either ABCB5 mAb-treated or isotype control-treated CRC cells cultured in the presence of recombinant IL-8. *C*, Western blot analyses of CDH1, CDH2, and VIM expression in either ABCB5 mAb–treated or isotype control mAb–treated CRC cells cultured in the presence of recombinant IL-8.

circulating ABCB5 mRNA is not expressed at significant levels in the peripheral blood of healthy humans (25) and, when detectable at significant levels in cancer patients, has been shown to arise from disseminated tumor cells (26, 47–49), suggesting that circulating ABCB5 mRNA detected in CRC patients in the current study similarly arose from tumor cell bloodstream invasion. Our findings in human-to-mouse CRC xenotransplantation models clearly support this notion, by documenting the functional role of ABCB5 in human CRC tumor cell blood stream invasion. Although we cannot rule out entirely that differences in primary tumor lesions may have influenced metastatic behavior in our experiments, such correlations between primary tumor size and the development of metastasis have not previously been observed in experimental cancer xenotransplantation models (30). Our results provide a rationale for future studies aimed at correlating circulating ABCB5 mRNA levels with the prognostic value of ABCB5(+) CTC numbers in CRC patients.

In summary, our finding that ABCB5 promotes tumor cell invasion in CRC suggests that novel ABCB5-targeted strategies in this malignancy might have the potential to disrupt two distinct but apparently related features of tumor aggressiveness (*i.e.* as previously shown, drug resistance (28), and, based on current results, invasive tumor progression).

Experimental procedures

Patients

This study prospectively enrolled patients undergoing treatment for CRC at the University Hospital of Würzburg from January 2003 to December 2008. Of 670 patients enrolled, 142 were included in this study based on the availability of histologically confirmed primary tumors or metastases and of pretreatment-obtained peripheral blood samples. Patient characteristics are summarized in Table S1. All patients were followed up regularly at 3–6-month intervals in accordance with the guidelines for the German Tumor Centers (completeness index of 0.96 (50)). Median follow-up in the data set for the CRC patients was 69 months (95% CI 62–73 months), which is based on a Kaplan–Meier estimate with an inverted censor. UICC stage I and stage II patients underwent surgical resection without adjuvant chemotherapy. Stage III colon cancer patients were treated with adjuvant chemotherapy (FOLFOX-4 or FOLOFOX-6 regimens) after surgical resection. Stage III rectal cancer patients were treated with neoadjuvant chemoradiation (two cycles of 5-fluorouracil with or without oxaliplatin and cumulative 54 grays of radiation before surgery followed by an additional four cycles of chemotherapy (FOLFOX-4 or FOLFOX-6 regimens) after the surgery. Stage IV patients were treated with several regimens (mostly FOLFOX or FOLFIRI with or without bevacizumab or cetuximab) with neoadjuvant or palliative intention to treat. The study was approved by the University Hospital of Würzburg Ethics Committee, and it abides by the Declaration of Helsinki principles. All patients enrolled in the study signed the informed consent.

Quantitative RT-PCR analyses

Peripheral blood (7.5 ml collected in EDTA-containing Vacutainers) was obtained from each patient before treatment initiation. After density centrifugation through Ficoll-Paque (Pharmacia, Freiburg, Germany; 30 min, 400 × *g*), peripheral mononuclear blood cells were harvested and washed twice in PBS. Cell pellets were snap-frozen in liquid nitrogen and stored at −80 °C until further use. mRNA was extracted from 1×10^6 cells using TRIzol reagent (Invitrogen, Darmstadt, Germany) according to the manufacturer's recommendations. cDNA synthesis was carried out using the iScript cDNA synthesis kit (Promega, Mannheim, Germany). The following primers were used: ABCB5 sense, 5′-CACAAAAGGCCATTCAGGCT-3′; ABCB5 antisense, 5′-GCTGAGGAATCCACCCAATCT-3′; β-actin sense, 5′-CCTGGCACCCAGCACAAT-3′; β-actin antisense, 5′-GCCGATCCACACGGAGTACT-3′. All PCRs were carried out with a DNA Engine Opticon 2 system (MJ Research, Biozym). Gene expression levels were normalized to β-actin and shown as Δ*Ct* calculated as *Ct* for the gene of interest minus *Ct* for β-actin.

For quantitative RT-PCR analyses of cultured CRC cells, total RNA was isolated using an RNeasy plus kit (Qiagen) as described previously (51). cDNA was synthesized from 1 μg of total RNA using the High-Capacity cDNA Reverse Transcription Kit with RNase Inhibitor (Invitrogen) according to the manufacturer's protocol. Quantitative RT-PCR was performed using the TaqMan® Gene Expression Master Mix (AB Applied Biosystems) with primers and TaqMan probes listed as follows: *CDH1* (Hs01013953), *CDH2* (Hs00983061), *VIM* (Hs00958112), *GAPDH* (Hs99999905), *B2M* (Hs00187842), *PPIA* (Hs99999904), *MRPL19* (Hs00608519), and *ACTB* (4352341E). All PCRs were carried out with a GeneAmp 7000 sequence detection system (Applied Biosystems) and assessed as described previously (52).

Cell culture

The authenticated human CRC cell lines HCT116, HT29, and SW620 were obtained from American Type Culture Collection. The authenticated human CRC cell line COLO741 was purchased from Sigma-Aldrich. Cells were cultured in RPMI 1640 medium (Lonza Bio-Whittaker) supplemented with 10% (v/v) fetal bovine serum (FBS) (Invitrogen Gibco) and 1% (v/v) penicillin/streptomycin (Lonza Bio-Whittaker).

Generation of stable knockdown and overexpressing colorectal cancer cell lines

Generation of stable COLO741 ABCB5-KD or control cell lines was accomplished by retroviral infection followed by puromycin selection (1 μg/ml). Briefly, using FuGENE HD Transfection Reagent, 293T cells were co-transfected with a retroviral vector pSMP expressing an shRNA of interest, a plasmid pCMV-Gag-Pol expressing the retroviral structure proteins, and a plasmid mediating viral entry. Retroviral stocks were collected as culture supernatants 48 h post-transfection and used for infection of COLO741 cells. The ABCB5 shRNA target sequence 5′-CCTCGAAGAAAGCACAGATTA-3′ was chosen among other targets tested based on the highest ABCB5-knockdown efficiency. The ABCB5 mRNA knockdown efficiency was confirmed by TaqMan® gene expression assays (Life Technologies, Inc., Hs00698751_m1) using GAPDH as the internal control (Life Technologies, Hs99999905_m1). Reduction of ABCB5 protein expression in ABCB5-KD cell lines was confirmed by flow cytometry. Stable COLO741 ABCB5-KD AXL–overexpressing and COLO741 ABCB5-KD–control cell lines were generated by transfection of plasmids pCMV-AXL and pCMV-entry (Origene), using FuGENE HD transfection reagent. Stably transfected cell clones were selected using Geneticin (1 mg/ml). AXL overexpression was confirmed at the mRNA level by qPCR using TaqMan® gene expression assays (Life Technologies, Hs01064445_m1), using GAPDH as internal control (Life Technologies, Hs99999905_m1). AXL protein expression was examined by Western blot analyses using goat anti-AXL polyclonal antibody.

Generation of a metastatic CRC cell pool COLO741MET

COLO741 cells were xenografted subcutaneously into the right flanks of recipient NSG mice (1×10^6/inoculum). At 8 weeks after tumor cell inoculation, mice were euthanized, and lung metastases were isolated under a dissecting microscope. The tissues were minced and digested in PBS containing 5 mg/ml collagenase IV (Worthington), 1 mM $CaCl_2$, 1% (v/v) penicillin/streptomycin (Lonza Bio-Whittaker), and 1% (v/v) antibiotic-antimycotic (Invitrogen Gibco) at 37 °C for 1 h with constant shaking at 250 rpm. Cells were filtered through a 40-μm cell strainer (BD Falcon), pelleted, washed twice with PBS, and transferred to 25-cm^2 culture flasks. Dissociated cell

cultures were incubated at 37 °C with 5% CO_2 in RPMI 1640 medium (Lonza Bio-Whittaker) supplemented with 10% (v/v) FBS (Invitrogen Gibco) and 1% (v/v) penicillin/streptomycin (Lonza Bio-Whittaker). The cells were passaged every 2–3 days and subjected to controlled trypsinizations to remove any contaminating fibroblasts.

Antibodies

The following primary antibodies were used in flow cytometry experiments: mouse monoclonal anti-ABCB5 antibody (clone 3C2-1D12) (17, 25, 31, 37, 51, 53) and anti-AXL polyclonal goat antibody (R&D Systems). MOPC-31C mouse isotype (BD Pharmingen) and polyclonal goat IgG (R&D Systems) were used as primary control antibodies. The secondary antibodies were rat anti-mouse IgG1-APC antibody (BD Pharmingen) and donkey anti-goat IgG-PE (R&D Systems). For the Western blots, the following antibodies were purchased from R&D Systems: human AXL polyclonal goat antibody, goat anti-rabbit IgG-HRP affinity-purified polyclonal antibody, goat anti-mouse IgG-HRP affinity-purified polyclonal antibody, and rabbit anti-goat IgG-HRP affinity-purified polyclonal antibody. In addition, the following antibodies were purchased from Cell Signaling Technology: β-actin (D6A8) rabbit mAb, E-cadherin (24E10) rabbit mAb, vimentin (D21H3) rabbit mAb, and N-cadherin (D4R1H) rabbit mAb. The following antibodies were used for functional ABCB5 inhibition studies: mouse monoclonal anti-ABCB5 antibody (clone 3C2-1D12) (25) and isotype control mAb (clone MOPC31C, Sigma).

Transwell in vitro invasion assays

The effect of ABCB5 on cell invasion was determined using BioCoat™ Matrigel® invasion chambers (Corning, Inc.) according to the manufacturer's instructions. Briefly, cells were seeded on the Matrigel-coated upper inserts in serum-free RPMI 1640 medium at a density of 5×10^4 cells/well for the COLO741, COLO741MET, COLO741MET CONTROL, and COLO741MET ABCB5-KD lines and of 2×10^5 cells/well for the SW620 line. The bottom wells were filled with 10% FBS-containing medium. For mAb-mediated ABCB5 blockade, isotype control mAb or anti-ABCB5 mAb was added fresh daily to both the upper and lower chambers at a concentration of 50 μg/ml. All studies were conducted in triplicates. After 24 or 48 h of incubation, the inserts were removed, and cells invading the lower chamber were stained with the Diff-Quik™ kit (Andwin Scientific, North Carolina, IL). The cells were photographed at ×10 magnification under a Nikon Eclipse TI microscope and counted in four randomly selected microscopic fields per well.

In vivo cell invasion assays

For *in vivo* cellular invasion analyses, we utilized a human-to-mouse xenotransplantation model as described previously (48). COLO741 and COLO741MET, as well as COLO741MET CONTROL and COLO741MET ABCB5-KD cells, were xenografted subcutaneously into the right flanks of recipient NSG mice (1×10^6/inoculum, $n = 8$ mice/group). At 8 weeks post-transplantation, mice were euthanized, and blood specimens were collected by cardiac puncture (48). Erythrocytes were lysed using the modified hypotonic shock method described previously (54). Briefly, 8.2 ml of ice-cold distilled water was added to 800 μl of the murine blood at 4 °C. The tubes were lightly agitated for 15 s, and then 1 ml of ice-cold 10× PBS was added to restore the isotonicity of the blood sample. After that, cell suspensions were centrifuged at 250 × *g* for 5 min at 4 °C to pellet the cells. The cell pellets were washed twice with ice-cold 1× PBS, resuspended in 1× RLT-plus buffer (Qiagen) containing 1% (v/v) β-mercaptoethanol, and stored at −80 °C for further analysis.

Flow cytometry

Cells were harvested using Versene (Invitrogen), passed through a 40-μm nylon mesh to exclude aggregates, and examined using trypan blue for cell viability as described previously (52). Analysis of ABCB5 and AXL expression was done by single-color flow cytometry as described previously (52).

Western blots

Protein lysates from cultured cells were prepared using 10× cell lysis buffer (Cell Signaling) supplemented with 1× complete protease inhibitor mixture (Roche Applied Science). For tumor tissues, total protein was purified using the AllPrep DNA/RNA/protein minikit (Qiagen). Immunoblotting was performed as described previously (51). Semiquantitative analysis of Western blots was performed using the software Image Studio Lite (LI-COR).

IL-8 ELISA and IL-8 rescue assays

Supernatants from CRC cell cultures treated with either isotype control or anti-ABCB5 mAb were collected, centrifuged to remove particulates, aliquoted, and stored at −80 °C before analysis. IL-8 concentration was measured using the human CXCL8/IL-8 Quantikine ELISA kit (R&D Systems) according to the manufacturer's instructions. For IL-8 rescue experiments, CRC cells were cultured in the presence of either vehicle control or recombinant IL-8 (R&D Systems) at the indicated concentrations for 72 h.

Animals

Immunodeficient male and female NOD.Cg-*Prkdc*^{scid} *Il2rg*^{tm1Wjl}/SzJ (NSG) mice were purchased from Jackson Laboratory. All animals were maintained in accordance with the institutional guidelines of the Veterans Affairs Boston Healthcare System, Harvard Medical School.

Statistical methods

For the clinical study, ABCB5 expression was summarized according to patient demographic or disease characteristics using the Wilcoxon rank-sum test (two categories) or the Kruskal–Wallis test (three or more categories). ABCB5 mRNA expression levels were divided into four classes according to the quartiles of the distribution of expression values. The distributions of OS were summarized using the method of Kaplan–Meier with 95% CIs estimated using log (−log (end point)) methodology. Cox proportional hazards regression models were fit to each of the time-to-event outcomes. ABCB5 expression (quartiles) was included as an independent variable in all

Cox models related to that biomarker. Additional candidate-independent predictors were patient gender, tumor location, tumor grade (grades 1 and 2 *versus* 3), UICC stage, T stage, N stage, and M stage, and patient age divided at the median (66 years). Standard model-building techniques were used. Predictors were considered statistically significant and included in the final model if the Wald χ^2 p value was <0.05 or if the model fit was significantly improved by including a predictor with a p value between 0.05 and 0.065 based on a log-likelihood test. Spearman correlation coefficients were used to describe the relationships between expression levels of the four biomarkers. Comparisons of ABCB5 expression between patients with CRC and controls were based on Wilcoxon rank-sum tests. The OS, determined as time in months from treatment initiation to death from any cause was chosen as the end point definition. In other, nonclinical experimental studies, statistical differences between expression levels of markers or between surviving cell fractions were determined by using paired or unpaired t-tests where appropriate, with two-sided p values of $p < 0.05$ considered significant.

Author contributions—Q. G., M. H. F., M. G., and N. Y. F. designed the study; Q. G., T. G., G. B., B. J. W., G. G., P. B., N. C., J. M., and N. Y. F. performed the experiments; Q. G., T. G., A. G.-H., M. H. F., C. G. L, G. F. M., M. G., and N. Y. F. analyzed the results; J. S. G, B. N., Q. H., A. M. W.-G., and M. G. provided clinical specimens; A. G.-H. performed the statistical analyses; Q. G., T. G., M. H. F., M. G., and N. Y. F. wrote the manuscript.

References

1. Futreal, P. A., Coin, L., Marshall, M., Down, T., Hubbard, T., Wooster, R., Rahman, N., and Stratton, M. R. (2004) A census of human cancer genes. *Nat. Rev. Cancer* **4,** 177–183 CrossRef Medline
2. Vogelstein, B., and Kinzler, K. W. (2004) Cancer genes and the pathways they control. *Nat. Med.* **10,** 789–799 CrossRef Medline
3. Bruce, W. R., and Van Der Gaag, H. (1963) A quantitative assay for the number of murine lymphoma cells capable of proliferation *in vivo*. *Nature* **199,** 79–80 CrossRef Medline
4. Fidler, I. J., and Hart, I. R. (1982) Biological diversity in metastatic neoplasms: origins and implications. *Science* **217,** 998–1003 CrossRef Medline
5. Reya, T., Morrison, S. J., Clarke, M. F., and Weissman, I. L. (2001) Stem cells, cancer, and cancer stem cells. *Nature* **414,** 105–111 CrossRef Medline
6. Ricci-Vitiani, L., Lombardi, D. G., Pilozzi, E., Biffoni, M., Todaro, M., Peschle, C., and De Maria, R. (2007) Identification and expansion of human colon-cancer-initiating cells. *Nature* **445,** 111–115 CrossRef Medline
7. O'Brien, C. A., Pollett, A., Gallinger, S., and Dick, J. E. (2007) A human colon cancer cell capable of initiating tumour growth in immunodeficient mice. *Nature* **445,** 106–110 CrossRef Medline
8. Zhu, L., Gibson, P., Currle, D. S., Tong, Y., Richardson, R. J., Bayazitov, I. T., Poppleton, H., Zakharenko, S., Ellison, D. W., and Gilbertson, R. J. (2009) Prominin 1 marks intestinal stem cells that are susceptible to neoplastic transformation. *Nature* **457,** 603–607 CrossRef Medline
9. Dean, M., Fojo, T., and Bates, S. (2005) Tumour stem cells and drug resistance. *Nat. Rev. Cancer* **5,** 275–284 CrossRef Medline
10. Mani, S. A., Guo, W., Liao, M. J., Eaton, E. N., Ayyanan, A., Zhou, A. Y., Brooks, M., Reinhard, F., Zhang, C. C., Shipitsin, M., Campbell, L. L., Polyak, K., Brisken, C., Yang, J., and Weinberg, R. A. (2008) The epithelial-mesenchymal transition generates cells with properties of stem cells. *Cell* **133,** 704–715 CrossRef Medline
11. Thiery, J. P. (2002) Epithelial-mesenchymal transitions in tumour progression. *Nat. Rev. Cancer* **2,** 442–454 CrossRef Medline
12. Frank, N. Y., Schatton, T., and Frank, M. H. (2010) The therapeutic promise of the cancer stem cell concept. *J. Clin. Invest.* **120,** 41–50 CrossRef Medline
13. Wilson, B. J., Saab, K. R., Ma, J., Schatton, T., Pütz, P., Zhan, Q., Murphy, G. F., Gasser, M., Waaga-Gasser, A. M., Frank, N. Y., and Frank, M. H. (2014) ABCB5 maintains melanoma-initiating cells through a proinflammatory cytokine signaling circuit. *Cancer Res.* **74,** 4196–4207 CrossRef Medline
14. Kugimiya, N., Nishimoto, A., Hosoyama, T., Ueno, K., Enoki, T., Li, T. S., and Hamano, K. (2015) The c-MYC-ABCB5 axis plays a pivotal role in 5-fluorouracil resistance in human colon cancer cells. *J. Cell. Mol. Med.* **19,** 1569–1581 CrossRef Medline
15. Yang, G., Jiang, O., Ling, D., Jiang, X., Yuan, P., Zeng, G., Zhu, J., Tian, J., Weng, Y., and Wu, D. (2015) MicroRNA-522 reverses drug resistance of doxorubicin-induced HT29 colon cancer cell by targeting ABCB5. *Mol. Med. Rep.* **12,** 3930–3936 CrossRef Medline
16. Wilson, B. J., Schatton, T., Zhan, Q., Gasser, M., Ma, J., Saab, K. R., Schanche, R., Waaga-Gasser, A. M., Gold, J. S., Huang, Q., Murphy, G. F., Frank, M. H., and Frank, N. Y. (2011) ABCB5 identifies a therapy-refractory tumor cell population in colorectal cancer patients. *Cancer Res.* **71,** 5307–5316 CrossRef Medline
17. Ksander, B. R., Kolovou, P. E., Wilson, B. J., Saab, K. R., Guo, Q., Ma, J., McGuire, S. P., Gregory, M. S., Vincent, W. J., Perez, V. L., Cruz-Guilloty, F., Kao, W. W., Call, M. K., Tucker, B. A., Zhan, Q., *et al.* (2014) ABCB5 is a limbal stem cell gene required for corneal development and repair. *Nature* **511,** 353–357 CrossRef Medline
18. Huang, E. H., Hynes, M. J., Zhang, T., Ginestier, C., Dontu, G., Appelman, H., Fields, J. Z., Wicha, M. S., and Boman, B. M. (2009) Aldehyde dehydrogenase 1 is a marker for normal and malignant human colonic stem cells (SC) and tracks SC overpopulation during colon tumorigenesis. *Cancer Res.* **69,** 3382–3389 CrossRef Medline
19. Kemper, K., Prasetyanti, P. R., De Lau, W., Rodermond, H., Clevers, H., and Medema, J. P. (2012) Monoclonal antibodies against Lgr5 identify human colorectal cancer stem cells. *Stem Cells* **30,** 2378–2386 CrossRef Medline
20. Powell, A. E., Wang, Y., Li, Y., Poulin, E. J., Means, A. L., Washington, M. K., Higginbotham, J. N., Juchheim, A., Prasad, N., Levy, S. E., Guo, Y., Shyr, Y., Aronow, B. J., Haigis, K. M., Franklin, J. L., and Coffey, R. J. (2012) The pan-ErbB negative regulator Lrig1 is an intestinal stem cell marker that functions as a tumor suppressor. *Cell* **149,** 146–158 CrossRef Medline
21. Chen, J., Xia, Q., Jiang, B., Chang, W., Yuan, W., Ma, Z., Liu, Z., and Shu, X. (2015) Prognostic value of cancer stem cell marker ALDH1 expression in colorectal cancer: a systematic review and meta-analysis. *PLoS One* **10,** e0145164 CrossRef Medline
22. Chen, Q., Zhang, X., Li, W. M., Ji, Y. Q., Cao, H. Z., and Zheng, P. (2014) Prognostic value of LGR5 in colorectal cancer: a meta-analysis. *PLoS One* **9,** e107013 CrossRef Medline
23. Chen, S., Song, X., Chen, Z., Li, X., Li, M., Liu, H., and Li, J. (2013) CD133 expression and the prognosis of colorectal cancer: a systematic review and meta-analysis. *PLoS One* **8,** e56380 CrossRef Medline
24. Visvader, J. E., and Lindeman, G. J. (2008) Cancer stem cells in solid tumours: accumulating evidence and unresolved questions. *Nat. Rev. Cancer* **8,** 755–768 CrossRef Medline
25. Frank, N. Y., Pendse, S. S., Lapchak, P. H., Margaryan, A., Shlain, D., Doeing, C., Sayegh, M. H., and Frank, M. H. (2003) Regulation of progenitor cell fusion by ABCB5 P-glycoprotein, a novel human ATP-binding cassette transporter. *J. Biol. Chem.* **278,** 47156–47165 CrossRef Medline
26. Reid, A. L., Millward, M., Pearce, R., Lee, M., Frank, M. H., Ireland, A., Monshizadeh, L., Rai, T., Heenan, P., Medic, S., Kumarasinghe, P., and Ziman, M. (2013) Markers of circulating tumour cells in the peripheral blood of patients with melanoma correlate with disease recurrence and progression. *Br. J. Dermatol.* **168,** 85–92 CrossRef Medline
27. Kheirelseid, E. A., Chang, K. H., Newell, J., Kerin, M. J., and Miller, N. (2010) Identification of endogenous control genes for normalisation of

real-time quantitative PCR data in colorectal cancer. *BMC Mol. Biol.* **11,** 12 CrossRef Medline
28. Wilson, B. J., Schatton, T., Frank, M. H., and Frank, N. Y. (2011) Colorectal cancer stem cells: biology and therapeutic implications. *Curr. Colorectal Cancer Rep.* **7,** 128–135 CrossRef Medline
29. Wolmark, N., Cruz, I., Redmond, C. K., Fisher, B., and Fisher, E. R. (1983) Tumor size and regional lymph node metastasis in colorectal cancer: a preliminary analysis from the NSABP clinical trials. *Cancer* **51,** 1315–1322 CrossRef Medline
30. Quintana, E., Piskounova, E., Shackleton, M., Weinberg, D., Eskiocak, U., Fullen, D. R., Johnson, T. M., and Morrison, S. J. (2012) Human melanoma metastasis in NSG mice correlates with clinical outcome in patients. *Sci. Transl. Med.* **4,** 159ra149 Medline
31. Frank, N. Y., Margaryan, A., Huang, Y., Schatton, T., Waaga-Gasser, A. M., Gasser, M., Sayegh, M. H., Sadee, W., and Frank, M. H. (2005) ABCB5-mediated doxorubicin transport and chemoresistance in human malignant melanoma. *Cancer Res.* **65,** 4320–4333 CrossRef Medline
32. Dunne, P. D., McArt, D. G., Blayney, J. K., Kalimutho, M., Greer, S., Wang, T., Srivastava, S., Ong, C. W., Arthur, K., Loughrey, M., Redmond, K., Longley, D. B., Salto-Tellez, M., Johnston, P. G., and Van Schaeybroeck, S. (2014) AXL is a key regulator of inherent and chemotherapy-induced invasion and predicts a poor clinical outcome in early-stage colon cancer. *Clin. Cancer Res.* **20,** 164–175 CrossRef Medline
33. Gjerdrum, C., Tiron, C., Høiby, T., Stefansson, I., Haugen, H., Sandal, T., Collett, K., Li, S., McCormack, E., Gjertsen, B. T., Micklem, D. R., Akslen, L. A., Glackin, C., and Lorens, J. B. (2010) Axl is an essential epithelial-to-mesenchymal transition-induced regulator of breast cancer metastasis and patient survival. *Proc. Natl. Acad. Sci. U.S.A.* **107,** 1124–1129 CrossRef Medline
34. Asiedu, M. K., Beauchamp-Perez, F. D., Ingle, J. N., Behrens, M. D., Radisky, D. C., and Knutson, K. L. (2014) AXL induces epithelial-to-mesenchymal transition and regulates the function of breast cancer stem cells. *Oncogene* **33,** 1316–1324 CrossRef Medline
35. Fernando, R. I., Castillo, M. D., Litzinger, M., Hamilton, D. H., and Palena, C. (2011) IL-8 signaling plays a critical role in the epithelial-mesenchymal transition of human carcinoma cells. *Cancer Res.* **71,** 5296–5306 CrossRef Medline
36. Hwang, W. L., Yang, M. H., Tsai, M. L., Lan, H. Y., Su, S. H., Chang, S. C., Teng, H. W., Yang, S. H., Lan, Y. T., Chiou, S. H., and Wang, H. W. (2011) SNAIL regulates interleukin-8 expression, stem cell-like activity, and tumorigenicity of human colorectal carcinoma cells. *Gastroenterology* **141,** 279–291, 291.e1–5 CrossRef Medline
37. Schatton, T., Murphy, G. F., Frank, N. Y., Yamaura, K., Waaga-Gasser, A. M., Gasser, M., Zhan, Q., Jordan, S., Duncan, L. M., Weishaupt, C., Fuhlbrigge, R. C., Kupper, T. S., Sayegh, M. H., and Frank, M. H. (2008) Identification of cells initiating human melanomas. *Nature* **451,** 345–349 CrossRef Medline
38. Cheung, S. T., Cheung, P. F., Cheng, C. K., Wong, N. C., and Fan, S. T. (2011) Granulin-epithelin precursor and ATP-dependent binding cassette (ABC)B5 regulate liver cancer cell chemoresistance. *Gastroenterology* **140,** 344–355 CrossRef Medline
39. Chartrain, M., Riond, J., Stennevin, A., Vandenberghe, I., Gomes, B., Lamant, L., Meyer, N., Gairin, J. E., Guilbaud, N., and Annereau, J. P. (2012) Melanoma chemotherapy leads to the selection of ABCB5-expressing cells. *PLoS One* **7,** e36762 CrossRef Medline
40. Bates, R. C., DeLeo, M. J., 3rd, Mercurio, A. M. (2004) The epithelial-mesenchymal transition of colon carcinoma involves expression of IL-8 and CXCR-1-mediated chemotaxis. *Exp. Cell Res.* **299,** 315–324 CrossRef Medline
41. Zhang, Z., Lee, J. C., Lin, L., Olivas, V., Au, V., LaFramboise, T., Abdel-Rahman, M., Wang, X., Levine, A. D., Rho, J. K., Choi, Y. J., Choi, C. M., Kim, S. W., Jang, S. J., Park, Y. S., *et al.* (2012) Activation of the AXL kinase causes resistance to EGFR-targeted therapy in lung cancer. *Nat. Genet.* **44,** 852–860 CrossRef Medline
42. Meyer, A. S., Miller, M. A., Gertler, F. B., and Lauffenburger, D. A. (2013) The receptor AXL diversifies EGFR signaling and limits the response to EGFR-targeted inhibitors in triple-negative breast cancer cells. *Sci. Signal.* **6,** ra66 Medline
43. Liu, Y. N., Chang, T. H., Tsai, M. F., Wu, S. G., Tsai, T. H., Chen, H. Y., Yu, S. L., Yang, J. C., and Shih, J. Y. (2015) IL-8 confers resistance to EGFR inhibitors by inducing stem cell properties in lung cancer. *Oncotarget* **6,** 10415–10431 Medline
44. Meyerhardt, J. A., and Mayer, R. J. (2005) Systemic therapy for colorectal cancer. *N. Engl. J. Med.* **352,** 476–487 CrossRef Medline
45. Kopetz, S., Chang, G. J., Overman, M. J., Eng, C., Sargent, D. J., Larson, D. W., Grothey, A., Vauthey, J. N., Nagorney, D. M., and McWilliams, R. R. (2009) Improved survival in metastatic colorectal cancer is associated with adoption of hepatic resection and improved chemotherapy. *J. Clin. Oncol.* **27,** 3677–3683 CrossRef Medline
46. Bennouna, J., Sastre, J., Arnold, D., Österlund, P., Greil, R., Van Cutsem, E., von Moos, R., Viéitez, J. M., Bouché, O., Borg, C., Steffens, C. C., Alonso-Orduna, V., Schlichting, C., Reyes-Rivera, I., Bendahmane, B., *et al.* (2013) Continuation of bevacizumab after first progression in metastatic colorectal cancer (ML18147): a randomised phase 3 trial. *Lancet Oncol.* **14,** 29–37 CrossRef Medline
47. Aya-Bonilla, C., Camilleri, E., Haupt, L. M., Lea, R., Gandhi, M. K., and Griffiths, L. R. (2014) *In silico* analyses reveal common cellular pathways affected by loss of heterozygosity (LOH) events in the lymphomagenesis of Non-Hodgkin's lymphoma (NHL). *BMC Genomics* **15,** 390 CrossRef Medline
48. Ma, J., Lin, J. Y., Alloo, A., Wilson, B. J., Schatton, T., Zhan, Q., Murphy, G. F., Waaga-Gasser, A. M., Gasser, M., Stephen Hodi, F., Frank, N. Y., and Frank, M. H. (2010) Isolation of tumorigenic circulating melanoma cells. *Biochem. Biophys. Res. Commun.* **402,** 711–717 CrossRef Medline
49. Gray, E. S., Reid, A. L., Bowyer, S., Calapre, L., Siew, K., Pearce, R., Cowell, L., Frank, M. H., Millward, M., and Ziman, M. (2015) Circulating melanoma cell subpopulations: their heterogeneity and differential responses to treatment. *J. Invest. Dermatol.* **135,** 2040–2048 CrossRef Medline
50. Schmiegel, W., Pox, C., Reinacher-Schick, A., Adler, G., Arnold, D., Fleig, W., Fölsch, U. R., Frühmorgen, P., Graeven, U., Heinemann, V., Hohenberger, W., Holstege, A., Junginger, T., Kopp, I., Kühlbacher, T., *et al.* (2010) S3 guidelines for colorectal carcinoma: results of an evidence-based consensus conference on February 6/7, 2004 and June 8/9, 2007 (for the topics IV, VI and VII). *Z. Gastroenterol.* **48,** 65–136 CrossRef Medline
51. Frank, N. Y., Schatton, T., Kim, S., Zhan, Q., Wilson, B. J., Ma, J., Saab, K. R., Osherov, V., Widlund, H. R., Gasser, M., Waaga-Gasser, A. M., Kupper, T. S., Murphy, G. F., and Frank, M. H. (2011) VEGFR-1 expressed by malignant melanoma initiating cells is required for tumor growth. *Cancer Res.* **71,** 1474–1485 CrossRef Medline
52. Frank, N. Y., Kho, A. T., Schatton, T., Murphy, G. F., Molloy, M. J., Zhan, Q., Ramoni, M. F., Frank, M. H., Kohane, I. S., and Gussoni, E. (2006) Regulation of myogenic progenitor proliferation in human fetal skeletal muscle by BMP4 and its antagonist Gremlin. *J. Cell Biol.* **175,** 99–110 CrossRef Medline
53. Civenni, G., Walter, A., Kobert, N., Mihic-Probst, D., Zipser, M., Belloni, B., Seifert, B., Moch, H., Dummer, R., van den Broek, M., and Sommer, L. (2011) Human CD271-positive melanoma stem cells associated with metastasis establish tumor heterogeneity and long-term growth. *Cancer Res.* **71,** 3098–3109 CrossRef Medline
54. Vuorte, J., Jansson, S. E., and Repo, H. (2001) Evaluation of red blood cell lysing solutions in the study of neutrophil oxidative burst by the DCFH assay. *Cytometry* **43,** 290–296 CrossRef Medline